

Strongly correlated Fermi superfluid near an orbital Feshbach resonance: Stability, equation of state and Leggett mode

Lianyi He¹, Jia Wang², Shi-Guo Peng^{2,3}, Xia-Ji Liu², and Hui Hu²

¹*State Key Laboratory of Low-Dimensional Quantum Physics and Collaborative Innovation Center for Quantum Matter, Department of Physics, Tsinghua University, Beijing 100084, China*

²*Centre for Quantum and Optical Science, Swinburne University of Technology, Melbourne 3122, Australia and*

³*State Key Laboratory of Magnetic Resonance and Atomic and Molecular Physics, Wuhan Institute of Physics and Mathematics, Chinese Academy of Science, Wuhan 430071, China*

(Dated: December 3, 2024)

We theoretically study the superfluid phase of a strongly correlated ^{173}Yb Fermi gas near its orbital Feshbach resonance, by developing a quantitative pair-fluctuation theory within a two-band model. We examine the density excitation spectrum of the system and determine a stability phase diagram. We find that the ^{173}Yb Fermi gas is intrinsically metastable and has a novel equation of state, due to the small but positive singlet scattering length. The massive Leggett mode, arising from the fluctuation of the relative phase of two order parameters, is severely damped. We discuss the parameter space where an undamped Leggett mode may exist.

PACS numbers: 03.75.Ss, 67.85.Lm

I. INTRODUCTION

The realization of magnetic Feshbach resonance (MFR) in alkali-metal atoms, i.e., tuning the s -wave scattering length of a two-component atomic Fermi gas using a magnetic field [1, 2], opens a new paradigm for studying strongly correlated many-body phenomena. The crossover from Bose-Einstein condensates (BEC) to Bardeen-Cooper-Schrieffer (BCS) superfluids [3] in both three [4–7] and two dimensions [8–12] has now been experimentally explored in greater detail, leading to a number of new concepts such as unitary fermionic superfluid and universal equation of state (EoS) [7, 13, 14] that bring new insights to better understand other strong interacting systems, including high- T_c superconductors [15], nuclear matter [16] and quark-gluon plasma [17].

For alkali-earth atoms (such as Sr) or alkali-earth-like atoms (i.e., Yb), however, the MFR mechanism does not work, due to their vanishing total electron spin [2]. In a recent pioneering work by R. Zhang *et al.* [18], an alternative mechanism of orbital Feshbach resonance (OFR) for ^{173}Yb atoms has been proposed. Thanks to a shallow bound state (i.e., a large triplet scattering length) caused by the inter-orbital (nuclear) spin-exchange interactions, the small difference in the nuclear Landé factor between different orbital states allows the tunability of scattering length through a magnetic field [18]. The existence of the predicted OFR has most recently been confirmed by either an anisotropic expansion [19] or a cross-thermalization measurement [20], which determined a resonance field $B_0 = 41 \pm 1\text{G}$ [19] or $B_0 = 55 \pm 8\text{G}$ [20, 21], respectively.

It is of great interest to explore the many-body physics of OFR. Indeed, there are a number of urgent problems to address. Earlier qualitative mean-field analysis introduced two order parameters and found that the OFR

is associated with the *out-of-phase* solution of the two pair potentials [18]. This solution is in fact an excited state (saddle point) in the landscape of the thermodynamic potential [22, 23], and therefore may suffer from the some instabilities encountered by the breached pairing or Sarma phase in imbalanced Fermi gases [24, 25]. On the other hand, the existence of two order parameters in OFR opens the possibility of observing the long-sought *massive* Leggett mode [26–29] resulted from the fluctuation of the relative phase of the two order parameters. More fascinatingly, OFR is a narrow resonance due to the significant closed-channel fraction [30]. Would we observe any novel feature of the EoS near the OFR of ^{173}Yb atoms?

In this work, we address those interesting questions on stability, equation of state and potential observation of the massive Leggett mode, and present a *quantitative* description of the zero-temperature superfluid state of ^{173}Yb atoms near OFR. Our main results are briefly summarized as follows (See also Fig. 1). (I) Our two-body calculation with realistic Lenard-Jones potentials predicts a resonance field $B_0 \simeq 39.4\text{G}$ (Fig. 1a), in good agreement with recent experimental observations [19, 20]. (II) There is a dynamical instability revealed by the density excitation spectrum (Fig. 1b). Fortunately, due to the small singlet scattering length, this instability occurs at very large momentum and hence is hard to trigger under current experimental conditions. In other words, the superfluid state of ^{173}Yb atoms with OFR is intrinsically metastable. (III) The small singlet scattering length also implies a novel EoS, which is peculiar for a Feshbach resonance with sizable closed-channel fraction. (IV) The massive Leggett mode in a ^{173}Yb Fermi gas is severely damped. An undamped Leggett mode may exist only for the case with both large singlet and triplet scattering lengths near the OFR resonance (Fig. 1b).

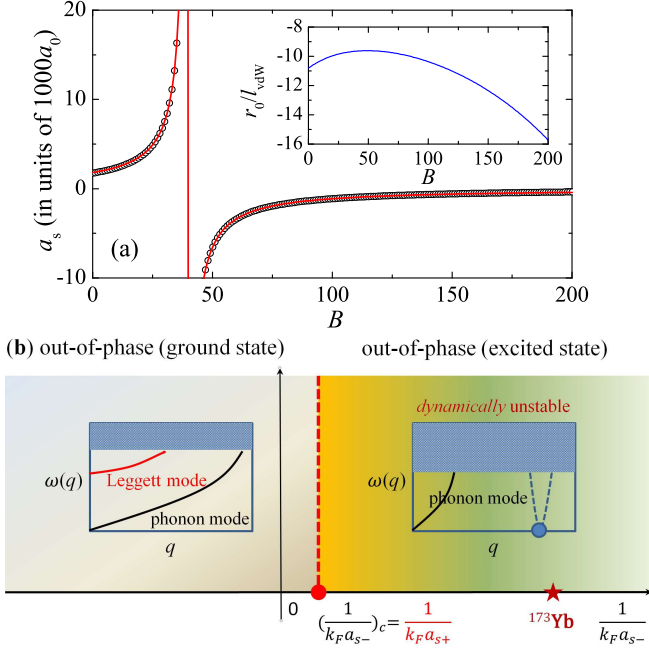


FIG. 1. (color online). (a) The scattering length a_s near the OFR of ^{173}Yb atoms. The circles are our two-body calculations and the red solid line is the fitting curve (see text). The inset shows the effective range near the same resonance. (b) An illustration of the many-body stability phase diagram. By tuning the interaction parameter $1/(k_F a_{s-})$ above a threshold $1/(k_F a_{s+})$, where a_{s-} and a_{s+} are the singlet and triplet scattering lengths, the out-of-phase solution - responsible for the OFR - develops an anomalous mode in its low-energy (density) excitation spectrum and is therefore dynamically unstable. In contrast, below the threshold, the out-of-phase solution is stable and may host an undamped Leggett mode.

II. TWO-BODY CALCULATION OF ^{173}Yb OFR

We start by briefly discussing the two-body physics for a Fermi gas of ^{173}Yb atoms with mass M in different electronic (orbital) states 1S_0 (denoted by $|g\sigma\rangle$) and 3P_0 ($|e\sigma'\rangle$), where σ and σ' stand for two nuclear spin states \uparrow, \downarrow . In the absence of magnetic field, a pair of atoms is well-described using the single $(-)$ or triplet $(+)$ basis:

$$|\pm\rangle = \frac{1}{2}(|ge\rangle \pm |eg\rangle) \otimes (|\uparrow\downarrow\rangle \mp |\downarrow\uparrow\rangle). \quad (1)$$

The interaction potentials are diagonal in this basis and are given by Lenard-Jones potentials,

$$V_{\pm}(r) = -\frac{C_6}{r^6} \left(1 - \frac{\alpha_{\pm}^6}{r^6}\right), \quad (2)$$

where $C_6 = 2561$ a.u. for ^{173}Yb [31] and α_{\pm} are the short-range parameters that are tuned to reproduce the singlet scattering length $a_{s-} \simeq 200a_0$ and the triplet scattering length $a_{s+} \simeq 1900a_0$ with a_0 being the Bohr radius [20]. In the presence of magnetic field, due to the slightly dif-

ferent Landé g -factor in two orbital states (i.e., $g_g \neq g_e$), it is more convenient to introduce a two-channel description, with the open- and closed-channel states given by

$$\begin{aligned} |o\rangle &= \frac{1}{\sqrt{2}}(|-\rangle + |+\rangle), \\ |c\rangle &= \frac{1}{\sqrt{2}}(|-\rangle - |+\rangle). \end{aligned} \quad (3)$$

One advantage of this new basis is that the Zeeman energy now becomes diagonal and their difference in the two channels is $\delta(B) = \delta\mu B$, where $\delta\mu = (g_e - g_g)(m_{\uparrow} - m_{\downarrow})\mu_B = 2\pi\hbar \times 112\Delta_m$ Hz/G with the Bohr magneton μ_B and $\Delta_m = 5$ [19, 20]. The key advantage, however, is the brilliant idea [18] that the scattering length in the open channel could be tuned by varying the detuning $\delta(B)$, exactly analogous to a MFR, provided that the bound-state energy in the closed channel is comparable to $\delta(B)$. This condition is generally impossible to satisfy, since $\delta(B)$ for nuclear spins is typically several order smaller in magnitude than that in a MFR. Luckily, for ^{173}Yb atoms, the *shallow* bound state due to the large triplet scattering length a_{s+} has the desired energy scale $\sim \delta(B)$.

The existence of such an OFR has been theoretically examined by using the pseudo-potential approach and the finite-range potential model [18]. In Ref. [20], by using a low-energy expansion of the singlet and triplet scattering phase shifts, where the effective ranges based on realistic potentials were included, the resonance field was predicted to be $B_0 \simeq 42\text{G}$. Here, we present a more realistic calculation by using the Lenard-Jones potential Eq. (2) and standard R -matrix propagation method [32], as shown in Fig. 1a. We find that the scattering observable in the open channel such as the scattering length a_s is not sensitive to α_{\pm} as long as $a_{s\pm}$ are reproduced. The calculated scattering length in the open channel is well fitted by a simple expression,

$$a_s = a_{bg} - \frac{\bar{a}\bar{E}s_{\text{res}}}{\delta\mu(B - B_0)}, \quad (4)$$

with the parameters

$$a_{bg} \simeq 29.96a_0, \quad s_{\text{res}} \simeq 0.154. \quad (5)$$

The resonance field B_0 is predicted to be

$$B_0 \simeq 39.4\text{G}. \quad (6)$$

Here, $\bar{a} \equiv [4\pi/\Gamma(1/4)^2]l_{\text{vdW}}$ and $\bar{E} = 1/(M\bar{a}^2)$ is the length and energy related to the van-der-Waals length $l_{\text{vdW}} \equiv (1/2)(MC_6)^{1/4} \simeq 84.8a_0$ and we set $\hbar = 1$. We find that the predicted resonance field $B_0 \simeq 39.4$ G agrees well with the experimental measurements [19, 20]. We note that, the small s_{res} implies that the OFR of ^{173}Yb atoms is a closed-channel dominated scattering [2].

III. EFFECTIVE FIELD THEORY OF OFR

The minimal model Hamiltonian for OFR can be given by $\mathcal{H} = \mathcal{H}_0 + \mathcal{H}_I$, where

$$\mathcal{H}_0 = \sum_{ni} \int d\mathbf{r} \psi_{ni}^\dagger(\mathbf{r}) \left(-\frac{\nabla^2}{2M} + \varepsilon_{ni} \right) \psi_{ni}(\mathbf{r}), \quad (7)$$

$$\mathcal{H}_I = \sum_{nm} \int d\mathbf{r} d\mathbf{r}' \varphi_n^\dagger(\mathbf{r}) V_{nm}(|\mathbf{r} - \mathbf{r}'|) \varphi_m(\mathbf{r}'). \quad (8)$$

Here $\varphi_n(\mathbf{r}) = \psi_{n2}(\mathbf{r})\psi_{n1}(\mathbf{r})$, and the subscript $n = o, c$ denotes the open or closed channel. The two internal degrees of freedom in each channel are indicated by $i = 1, 2$. Without loss of generality, the threshold energies ε_{ni} can be chosen as

$$\varepsilon_{o1} = \varepsilon_{o2} = 0, \quad \varepsilon_{c1} = \varepsilon_{c2} = \frac{1}{2}\delta(B). \quad (9)$$

The interaction potentials $V_{nm}(r)$ following the basis transformation of Eq. (2) read,

$$\begin{aligned} V_{oo}(r) &= V_{cc}(r) = \frac{1}{2}[V_-(r) + V_+(r)], \\ V_{oc}(r) &= V_{co}(r) = \frac{1}{2}[V_-(r) - V_+(r)]. \end{aligned} \quad (10)$$

The realistic form of the microscopic potential $V_{nm}(r)$ is rather hard for both the scattering problem and the many-body problem. The effective ranges r_\pm of the microscopic potentials $V_\pm(r)$ introduces an energy scale $\varepsilon_r \sim 1/(Mr_\pm^2)$. At low scattering energy $E = k^2/M \ll \varepsilon_r$, the shape of the microscopic interaction potentials $V_\pm(r)$ is not important. For many-body physics, this means that all kinds of short-ranged potentials $V_\pm(r)$ with the same scattering lengths $a_{s\pm}$ lead to the same prediction in the dilute limit. One way to simplify the calculation is to use the pseudo-potentials [18]

$$V_\pm(r) \simeq \frac{4\pi a_{s\pm}}{M} \delta(\mathbf{r}) \frac{\partial}{\partial r}(r\cdot), \quad (11)$$

or equivalently

$$\begin{aligned} V_{oo}(r) &= V_{cc}(r) \simeq \frac{4\pi a_{s0}}{M} \delta(\mathbf{r}) \frac{\partial}{\partial r}(r\cdot), \\ V_{oc}(r) &= V_{co}(r) \simeq \frac{4\pi a_{s1}}{M} \delta(\mathbf{r}) \frac{\partial}{\partial r}(r\cdot). \end{aligned} \quad (12)$$

Here the scattering lengths a_{s0} and a_{s1} are defined as

$$a_{s0} = \frac{1}{2}(a_{s-} + a_{s+}), \quad a_{s1} = \frac{1}{2}(a_{s-} - a_{s+}). \quad (13)$$

However, for the purpose of making use of the field theoretical approaches for the many-body problem, it is more convenient to employ the leading-order low-energy effective theory, i.e., the contact interaction potential. Therefore, we write

$$V_{nm}(|\mathbf{r} - \mathbf{r}'|) = V_{nm} \delta(\mathbf{r} - \mathbf{r}'). \quad (14)$$

Here the contact couplings $V_{oo} = V_{cc}$ and $V_{oc} = V_{co}$ are bare quantities and should be renormalized by using the physical scattering lengths $a_{s\pm}$ or $a_{s0,1}$. By making use of the contact potentials, the Lippmann-Schwinger equation of the scattering T matrix becomes a simple algebra equation,

$$\begin{aligned} & \begin{pmatrix} T_{oo}(E) & T_{oc}(E) \\ T_{co}(E) & T_{cc}(E) \end{pmatrix}^{-1} \\ &= \begin{pmatrix} V_{oo} & V_{oc} \\ V_{co} & V_{cc} \end{pmatrix}^{-1} - \begin{pmatrix} \mathcal{B}_o(E) & 0 \\ 0 & \mathcal{B}_c(E) \end{pmatrix}, \end{aligned} \quad (15)$$

where the two-particle bubble functions are given by

$$\begin{aligned} \mathcal{B}_o(E) &= \sum_{\mathbf{p}} \frac{1}{E + i\epsilon - 2\varepsilon_{\mathbf{p}}}, \\ \mathcal{B}_c(E) &= \sum_{\mathbf{p}} \frac{1}{E + i\epsilon - \delta(B) - 2\varepsilon_{\mathbf{p}}} \end{aligned} \quad (16)$$

Here $\epsilon = 0^+$ and $\varepsilon_{\mathbf{p}} = \mathbf{p}^2/(2M)$. The cost of the contact interaction is that the integral over the fermion momentum \mathbf{p} becomes divergent. We introduce a cutoff Λ for $|\mathbf{p}|$ and obtain

$$\begin{aligned} \mathcal{B}_o(E) &= -\eta(\Lambda) + \Pi_o(E), \\ \mathcal{B}_c(E) &= -\eta(\Lambda) + \Pi_c(E), \end{aligned} \quad (17)$$

where the divergent pieces read

$$\eta(\Lambda) = \sum_{\mathbf{p}} \frac{1}{2\varepsilon_{\mathbf{p}}} = \frac{M\Lambda}{2\pi^2}. \quad (18)$$

The finite pieces are given by

$$\begin{aligned} \Pi_o(E) &= \frac{M}{4\pi} \sqrt{-M(E + i\epsilon)}, \\ \Pi_c(E) &= \frac{M}{4\pi} \sqrt{-M(E + i\epsilon - \delta)}. \end{aligned} \quad (19)$$

Physically, the UV cutoff Λ corresponds to the momentum scale of order of $O(1/r_\pm)$ and should be sent to infinity if we set $r_\pm \rightarrow 0$.

A. Renormalization

The UV divergence can be completely removed by renormalization of the bare contact coupling matrix V . The renormalized coupling matrix U are related to the bare coupling matrix through [33]

$$\begin{pmatrix} U_{oo} & U_{oc} \\ U_{co} & U_{cc} \end{pmatrix}^{-1} = \begin{pmatrix} V_{oo} & V_{oc} \\ V_{co} & V_{cc} \end{pmatrix}^{-1} + \eta(\Lambda) I_{2 \times 2}. \quad (20)$$

Therefore, we have

$$U_{oo} = U_{cc} \equiv U_0, \quad U_{oc} = U_{co} \equiv U_1. \quad (21)$$

Then the Lippmann-Schwinger equation becomes cutoff independent,

$$\begin{pmatrix} T_{oo}(E) & T_{oc}(E) \\ T_{co}(E) & T_{cc}(E) \end{pmatrix}^{-1} = \begin{pmatrix} U_0 & U_1 \\ U_1 & U_0 \end{pmatrix}^{-1} - \begin{pmatrix} \Pi_o(E) & 0 \\ 0 & \Pi_c(E) \end{pmatrix}. \quad (22)$$

Solving the Lippmann-Schwinger equation, we obtain the T matrix for the open channel,

$$T_{oo}^{-1}(E) = \left[U_0 + \frac{U_1^2 \Pi_c(E)}{1 - U_0 \Pi_c(E)} \right]^{-1} - \Pi_o(E). \quad (23)$$

To complete the contact potential description of the orbital Feshbach resonance, we finally need to relate the elements of the renormalized coupling matrix U to the physical quantities. To this end, we calculate open-channel scattering amplitude

$$f_o(k) = -\frac{M}{4\pi} T_{oo} \left(E = \frac{k^2}{M} \right). \quad (24)$$

It can be expressed as

$$f_o(k) = \frac{1}{k \cot \delta_s(k) - ik}, \quad (25)$$

where the effective s -wave scattering phase shift $\delta_s(k)$ is given by

$$k \cot \delta_s(k) = -\frac{1 - \frac{MU_0}{4\pi} \sqrt{M\delta - k^2}}{\frac{MU_0}{4\pi} - \left[\left(\frac{MU_0}{4\pi} \right)^2 - \left(\frac{MU_1}{4\pi} \right)^2 \right] \sqrt{M\delta - k^2}} \quad (26)$$

Matching this result to the known result from quantum mechanical calculation [18], we obtain

$$U_0 = \frac{4\pi a_{s0}}{M}, \quad U_1 = \frac{4\pi a_{s1}}{M}. \quad (27)$$

The effective s -wave scattering length of the open channel can be given by $a_s = -f_o(k=0)$. We obtain [18]

$$a_s = \frac{a_{s0} - (a_{s0}^2 - a_{s1}^2) \sqrt{M\delta}}{1 - a_{s0} \sqrt{M\delta}}. \quad (28)$$

Therefore, there exists a scattering resonance at $\delta = 1/(Ma_{s0}^2)$ if $a_{s0} > 0$ [18].

B. Bound states

The bound states or molecule states can be obtained by solving the poles of the off-shell T matrix $T(Z)$ with the on-shell scattering energy E replaced with the off-shell variable $Z = \omega - \mathbf{q}^2/(4M)$. Here ω and \mathbf{q} represents the energy and momentum of the two-body states, respectively. The bound states corresponds to the $Z < 0$ poles

of the following equation

$$\det \begin{pmatrix} T_{oo}(Z) & T_{oc}(Z) \\ T_{co}(Z) & T_{cc}(Z) \end{pmatrix}^{-1} = 0, \quad (29)$$

or explicitly,

$$\frac{1}{a_{s0}^2 - a_{s1}^2} - \frac{a_{s0}}{a_{s0}^2 - a_{s1}^2} \left[\sqrt{-MZ} + \sqrt{-M(Z - \delta)} \right] + \sqrt{-MZ} \sqrt{-M(Z - \delta)} = 0. \quad (30)$$

Since the OFR exist only if $a_{s0} > 0$, we set $a_{s0} > 0$ and hence the resonance point is $\delta_{\text{res}} = 1/(Ma_{s0}^2)$. By making use of δ_{res} , we can express the pole equation as

$$\frac{1 - \sqrt{-x} - \sqrt{-x + d}}{1 - t^2} + \sqrt{-x(-x + d)} = 0. \quad (31)$$

Here the dimensionless variables are defined as $x = Z/\delta_{\text{res}}$ and $d = \delta/\delta_{\text{res}}$. It is clear that the energy spectrum of the bound states depends solely on the ratio

$$t = \frac{a_{s1}}{a_{s0}} = \frac{a_{s-} - a_{s+}}{a_{s-} + a_{s+}}. \quad (32)$$

Since $a_{s0} > 0$ we can set $a_{s+} > 0$ without loss of generality. We have $a_{s-}/a_{s+} > -1$ and therefore $-\infty < t < 1$. We therefore find two cases for the bound state spectrum: (1) If $a_{s-} > 0$ and hence $-1 < t < 1$ or $t^2 < 1$, there exist two molecule states: One is the Feshbach molecule state, which exists at the BEC side of the resonance $0 < \delta < \delta_{\text{res}}$, and the other is a bound state below the Feshbach molecule state, which exists for all values of δ . A special case is $t = 0$ which means the two channels decouples. We have two solutions: $Z = -\delta_{\text{res}}$ which exists for all δ , and $Z = \delta - \delta_{\text{res}}$ which exists for $0 < \delta < \delta_{\text{res}}$. (2) If $a_{s-} < 0$ and hence $t < -1$ or $t^2 > 1$, the pole equation gives only one solution at the BEC side $0 < \delta < \delta_{\text{res}}$, corresponding the Feshbach molecule state.

To understand the above results (and also for the understanding of the many-body case), it is intuitive to take a look at the case $\delta = 0$. In this case, Eq. (31) can be simplified as

$$(1 \pm |t|) \sqrt{-x} = 1. \quad (33)$$

Therefore, for $|t| < 1$ or $a_{s-} > 0$, there exist two solutions

$$Z_{\pm}(0) = -\left(\frac{1}{1 \pm |t|} \right)^2 \delta_{\text{res}}. \quad (34)$$

For $|t| \rightarrow 1$, we have $|Z_{-}(0)| \gg |Z_{+}(0)|$ and hence the two bound state levels are well separated. In this case, the solution Z_{-} , which is almost a constant for all values of the detuning δ , corresponds to a deep bound state and may decouple from the BCS-BEC crossover physics. For ^{173}Yb atoms, we have $a_{s+} \simeq 1900a_0$ and $a_{s-} \simeq 200a_0$ and hence $t \simeq -0.81$. In this case, the two solutions are

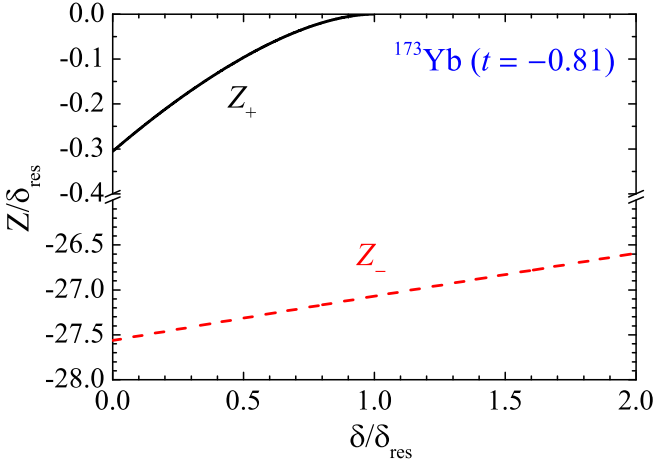


FIG. 2. (color online). Energy spectrum of the bound states across the OFR in ^{137}Yb atoms. The two energy levels, the Feshbach molecule state (Z_+) and the deep bound state (Z_-), are determined by Eq. (31).

given by

$$Z_{\pm}(0) = -\frac{1}{Ma_{s\pm}^2}. \quad (35)$$

Therefore, for ^{137}Yb atoms we have

$$\frac{|Z_-(0)|}{|Z_+(0)|} \simeq 90. \quad (36)$$

A full energy spectrum in the range $0 < \delta/\delta_{\text{res}} < 2$ is shown in Fig. 2. It is clear that a Feshbach molecule state (Z_+) exists in the BEC regime ($0 < \delta < \delta_{\text{res}}$). Another deep bound state Z_- exists for all values of δ .

IV. MANY-BODY THEORY OF FERMI GASES ACROSS AN OFR

The two-band model (7) that uses the singlet and triplet scattering lengths $a_{s\pm}$ as the input provides a *minimal* model to describe the many-body aspect of OFR [23, 33]. In the dilute limit, it agrees reasonably with the two-body calculation [18, 30], and within the mean-field approximation it captures the qualitative physics of superfluid pairings [18, 23]. Here, we consider *strong* pair fluctuations on top of the mean-field solution, which must be accounted for near OFR. The grand canonical Hamiltonian of the two-band model is given by

$$\begin{aligned} \mathcal{H} - \mu\mathcal{N} = & \sum_{ni} \int d\mathbf{r} \psi_{ni}^\dagger(\mathbf{r}) \left(-\frac{\nabla^2}{2M} - \mu_n \right) \psi_{ni}(\mathbf{r}) \\ & + \sum_{nm} V_{nm} \int d\mathbf{r} \varphi_n^\dagger(\mathbf{r}) \varphi_m(\mathbf{r}). \end{aligned} \quad (37)$$

Here μ is the chemical potential conjugated to the total particle number $\mathcal{N} = \sum_{ni} \int d\mathbf{r} \psi_{ni}^\dagger(\mathbf{r}) \psi_{ni}(\mathbf{r})$. The effective chemical potentials of the two channels are defined as

$$\mu_o = \mu, \quad \mu_c = \mu - \frac{1}{2}\delta(B). \quad (38)$$

We solve the two-band model Hamiltonian by using a functional path-integral approach [33–38]. The partition function of the many-body system can be expressed as

$$\mathcal{Z} = \int [d\psi][d\psi^\dagger] \exp(-\mathcal{S}), \quad (39)$$

where the action \mathcal{S} reads

$$\mathcal{S} = \int dx \sum_{ni} \psi_{ni}^\dagger(x) \partial_\tau \psi_{ni}(x) + \int_0^\beta d\tau (\mathcal{H} - \mu\mathcal{N}). \quad (40)$$

Here $x = (\tau, \mathbf{r})$ and $\int dx = \int_0^\beta d\tau \int d^3\mathbf{r}$, with τ being the imaginary time, and $\beta = 1/T$, with T being the temperature of the system and the Boltzmann constant $k_B = 1$. Following the standard field theoretical treatment, we introduce the auxiliary pairing fields

$$\Phi(x) = \begin{pmatrix} \Phi_o(x) \\ \Phi_c(x) \end{pmatrix} = \begin{pmatrix} V_{oo} & V_{oc} \\ V_{co} & V_{cc} \end{pmatrix} \begin{pmatrix} \varphi_o(x) \\ \varphi_c(x) \end{pmatrix}, \quad (41)$$

apply the Hubbard-Stratonovich transformation, and integrate out the fermion fields. The partition function of the system can be expressed as

$$\mathcal{Z} = \int [d\Phi][d\Phi^\dagger] \exp(-\mathcal{S}_{\text{eff}}). \quad (42)$$

The effective action \mathcal{S}_{eff} reads

$$\begin{aligned} \mathcal{S}_{\text{eff}} = & - \int dx \Phi^\dagger(x) V^{-1} \Phi(x) \\ & - \sum_{n=o,c} \text{Tr} \ln \mathbf{G}_n^{-1}[\Phi_n(x)], \end{aligned} \quad (43)$$

where the inverse fermion Green's functions are given by

$$\begin{aligned} \mathbf{G}_n^{-1} = & \begin{pmatrix} -\partial_\tau + \frac{\nabla^2}{2M} + \mu_n & \Phi_n(x) \\ \Phi_n^*(x) & -\partial_\tau - \frac{\nabla^2}{2M} - \mu_n \end{pmatrix} \\ & \times \delta(x - x'). \end{aligned} \quad (44)$$

In the superfluid phase, the pairing fields have nonzero expectation values. We write

$$\Phi_n(x) = \Delta_n + \phi_n(x), \quad (45)$$

where the uniform parts Δ_o and Δ_c serve as the order parameters of superfluidity. The effective action \mathcal{S}_{eff} can then be expanded about its mean-field solution, or in powers of the quantum fluctuations $\phi_o(x)$ and $\phi_c(x)$,

leading to [33–36]

$$\mathcal{S}_{\text{eff}}[\Phi, \Phi^*] = \mathcal{S}_{\text{MF}} + \mathcal{S}_{\text{GF}}[\phi, \phi^*] + \dots \quad (46)$$

Here \mathcal{S}_{MF} is the mean-field part, and $\mathcal{S}_{\text{GF}}[\phi, \phi^*]$ denotes the Gaussian fluctuation part which is quadratic in ϕ and ϕ^* . In the Gaussian pair fluctuation (GPF) theory, all the fluctuation contributions beyond Gaussian are neglected.

The mean-field contribution to the thermodynamic potential, $\Omega_{\text{MF}} = \mathcal{S}_{\text{MF}}/(\beta V)$, is given by

$$\Omega_{\text{MF}} = -\Delta^\dagger \begin{pmatrix} V_{\text{oo}} & V_{\text{oc}} \\ V_{\text{co}} & V_{\text{cc}} \end{pmatrix}^{-1} \Delta + \sum_{\mathbf{n}\mathbf{k}} (\xi_{\mathbf{n}\mathbf{k}} - E_{\mathbf{n}\mathbf{k}}), \quad (47)$$

where $\Delta \equiv (\Delta_o, \Delta_c)^T$ and the dispersions in each channel are defined as $\xi_{\mathbf{n}\mathbf{k}} = \varepsilon_{\mathbf{k}} - \mu_n$ and $E_{\mathbf{n}\mathbf{k}} = \sqrt{\xi_{\mathbf{n}\mathbf{k}}^2 + |\Delta_n|^2}$. By using the renormalized coupling matrix \bar{U} , we find that the UV divergence is completely removed. We obtain

$$\Omega_{\text{MF}} = -\Delta^\dagger \begin{pmatrix} \lambda_0 & \lambda_1 \\ \lambda_1 & \lambda_0 \end{pmatrix} \Delta + \sum_{\mathbf{n}\mathbf{k}} \left(\xi_{\mathbf{n}\mathbf{k}} - E_{\mathbf{n}\mathbf{k}} + \frac{\Delta_n^2}{2\varepsilon_{\mathbf{k}}} \right), \quad (48)$$

where

$$\lambda_0 = \frac{M}{4\pi} \frac{a_{s0}}{a_{s0}^2 - a_{s1}^2}, \quad \lambda_1 = -\frac{M}{4\pi} \frac{a_{s1}}{a_{s0}^2 - a_{s1}^2}. \quad (49)$$

In the GPF theory, the order parameters Δ_o and Δ_c as functions of the chemical potential μ should be determined by the stationary condition $\partial\Omega_{\text{MF}}/\partial\Delta_n = 0$, which gives rise to the so-called gap equation,

$$\begin{bmatrix} F_o(\Delta_o) & -\lambda_1 \\ -\lambda_1 & F_c(\Delta_c) \end{bmatrix} \begin{pmatrix} \Delta_o \\ \Delta_c \end{pmatrix} = 0, \quad (50)$$

where

$$F_n(\Delta_n) \equiv -\lambda_0 + \sum_{\mathbf{k}} \left(\frac{1}{2\varepsilon_{\mathbf{k}}} - \frac{1}{2E_{\mathbf{n}\mathbf{k}}} \right). \quad (51)$$

Note that Δ_o and Δ_c are complex quantities. Without loss of generality, we set Δ_o to be real and positive. From the gap equation (50), we find that Δ_c is also real. However, there may exist two kinds of solutions: an in-phase solution with $\Delta_c > 0$ and an out-of-phase solution with $\Delta_c < 0$. It is easy to show that for ^{173}Yb atoms, the out-of-phase solution is responsible for the BCS-BEC crossover, while the in-phase solution corresponds to the deep bound state. To show this, we take a look at $\delta = 0$ where the two channels become degenerate. In this case, we have $|\Delta_o| = |\Delta_c| \equiv \Delta$. For the out-of-phase solution, the gap equation becomes

$$\sum_{\mathbf{k}} \left[\frac{1}{2\varepsilon_{\mathbf{k}}} - \frac{1}{2\sqrt{(\varepsilon_{\mathbf{k}} - \mu)^2 + \Delta^2}} \right] = \frac{M}{4\pi a_{s+}}, \quad (52)$$

while for the in-phase solution, we obtain

$$\sum_{\mathbf{k}} \left[\frac{1}{2\varepsilon_{\mathbf{k}}} - \frac{1}{2\sqrt{(\varepsilon_{\mathbf{k}} - \mu)^2 + \Delta^2}} \right] = \frac{M}{4\pi a_{s-}}. \quad (53)$$

Comparing with the two-body result (35), we find that the in-phase solution corresponds to the deep bound state. For this solution, the chemical potential μ is large and negative for all values of the magnetic detuning δ . Therefore, even though the in-phase solution may be the true ground state of the Hamiltonian, it is a trivial solution which has nothing to do with the BCS-BEC crossover associate with the OFR.

The contribution from the Gaussian fluctuations to the thermodynamic potential can be worked out by completing the path integral over the fluctuations ϕ and ϕ^* . It can be expressed as

$$\Omega_{\text{GF}} = \frac{1}{2\beta} \sum_Q \ln \det [-\Gamma^{-1}(Q)], \quad (54)$$

where $Q \equiv (\mathbf{q}, i\nu_l)$ and $i\nu_l$ is the bosonic Matsubara frequencies, and the inverse vertex function (i.e., the Green function of collective modes) is,

$$-\Gamma^{-1}(Q) = \begin{bmatrix} M_{11}^o & M_{12}^o & -\lambda_1 & 0 \\ M_{21}^o & M_{22}^o & 0 & -\lambda_1 \\ -\lambda_1 & 0 & M_{11}^c & M_{12}^c \\ 0 & -\lambda_1 & M_{21}^c & M_{22}^c \end{bmatrix}, \quad (55)$$

with the matrix elements at zero temperature ($n = o, c$),

$$\begin{aligned} M_{11,C}^n(Q) &= \sum_{\mathbf{k}} \left(\frac{u_{n+}^2 u_{n-}^2}{i\nu_l - E_{n+} - E_{n-}} + \frac{1}{2\varepsilon_{\mathbf{k}}} \right) - \lambda_0, \\ M_{11}^n(Q) &= M_{11,C}^n(Q) - \sum_{\mathbf{k}} \frac{v_{n+}^2 v_{n-}^2}{i\nu_l + E_{n+} + E_{n-}}, \\ M_{12}^n(Q) &= \sum_{\mathbf{k}} \frac{\Delta_n^2}{2} \frac{1/E_{n+} + 1/E_{n-}}{(E_{n+} + E_{n-})^2 - (i\nu_l)^2}, \end{aligned} \quad (56)$$

and $M_{21}^n(Q) = M_{12}^n(Q)$, $M_{22}^n(Q) = M_{11}^n(-Q)$, and $M_{22,C}^n(Q) = M_{11,C}^n(-Q)$. Here, we use the short notations $E_{n\pm} \equiv E_{\mathbf{n}\mathbf{k}\pm\mathbf{q}/2}$, $u_{n\pm}^2 = (1 + \xi_{n\pm}/E_{n\pm})/2$ and $v_{n\pm}^2 = (1 - \xi_{n\pm}/E_{n\pm})/2$. The summation over the Matsubara frequencies $i\nu_l$ in Eq. (54) is generally divergent. Following the work by Diener *et al.* [36], we cure the divergence by subtracting a *vanishing* regular term $(k_B T/2) \sum_Q \ln \det [-\Gamma_C^{-1}(Q)]$, where $\Gamma_C^{-1}(Q)$ is obtained by replacing $M_{11}^n(Q)$ with $M_{11,C}^n(Q)$ and $M_{22}^n(Q)$ with $M_{22,C}^n(Q)$, and by setting $M_{12}^n(Q) = 0$ in $\Gamma^{-1}(Q)$. Finally, the convergent result can be expressed as

$$\Omega_{\text{GF}} = \frac{1}{2\beta} \sum_Q \ln \left\{ \frac{\det [-\Gamma^{-1}(Q)]}{\det [-\Gamma_C^{-1}(Q)]} \right\}. \quad (57)$$

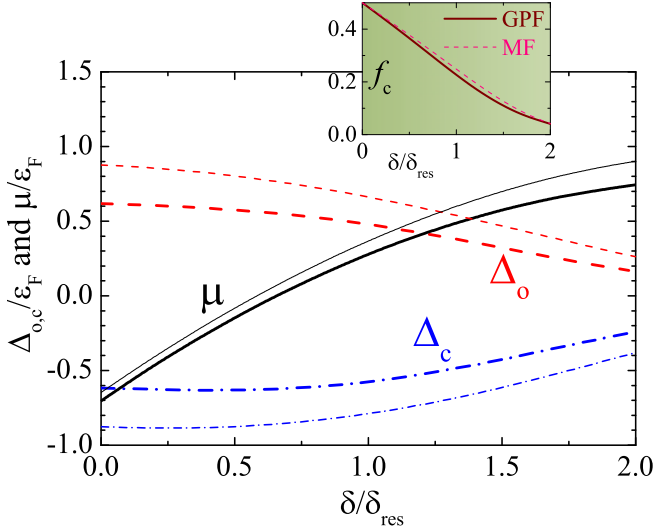


FIG. 3. (color online). The chemical potential and two gap parameters as a function of $\delta(B)$ at $T = 0$. For comparison, the mean-field predictions are shown by the thin lines. The inset shows the detuning dependence of the closed-channel fraction $f_c = n_c/n$.

In the absence of the inter-channel coupling parameter, i.e., $U_1 = 0$ or $\lambda_1 = 0$, our GPF equations reduce to describe two separate BEC-BCS crossover Fermi gases in the open and closed channels. In the unitary limit ($\lambda_0 = 0$), it is known that for each channel the GPF theory predicts accurate zero-temperature equation of state within a few percent relative error [35, 36], compared with the latest experimental measurements [5, 7]. At nonzero λ_1 , similarly, the GPF theory would be quantitatively reliable. To solve the EoS at a given detuning $\delta(B)$, we adjust the chemical potential μ to satisfy the number equation [35–38]

$$n = -\frac{\partial(\Omega_{\text{MF}} + \Omega_{\text{GF}})}{\partial\mu}, \quad (58)$$

and then calculate the pressure $P = -(\Omega_{\text{MF}} + \Omega_{\text{GF}})$, compressibility $\kappa = (1/n^2)(\partial n/\partial\mu)$, and the speed of sound $c_s = \sqrt{n/[m\partial n/\partial\mu]}$. Throughout the Letter, we take $n = 5 \times 10^{13} \text{ cm}^{-3}$, the typical peak density for ^{173}Yb atoms [19, 20], and $k_F = (3\pi^2 n)^{1/3} \simeq 1.14 \times 10^5 \text{ cm}^{-1}$, unless otherwise specified. We focus on the *out-of-phase* solution, which is responsible to the BCS-BEC crossover associate with the OFR [18, 23].

The solution of ^{173}Yb atoms from the mean-field theory (MF) or Gaussian-pair-fluctuation theory (GPF) is shown in Fig. 3, as a function of the detuning $\delta(B)$ in units of $\delta_{\text{res}} = 1/(Ma_{s0}^2)$ [18]. The quantitative improvement of our GPF theory over mean-field is evident and should be observable in future experiments. Near OFR, the closed-channel fraction is always significant (see the inset), indicating that the resonantly interacting super-

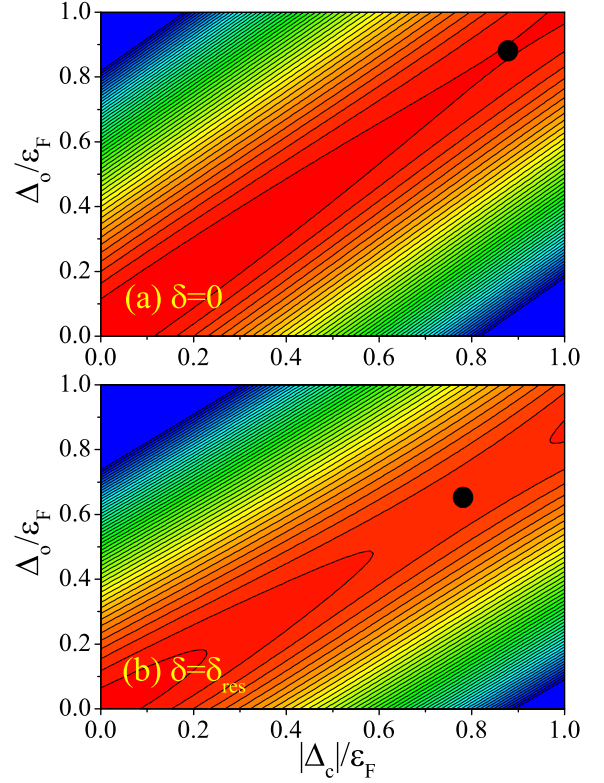


FIG. 4. (color online). Contour plots of the mean-field grand potential $\Omega_{\text{MF}}(\Delta_o, \Delta_c)$ near the out-of-phase solution ($\Delta_o > 0$ and $\Delta_c < 0$) for $\delta = 0$ (a) and $\delta = \delta_{\text{res}}$ (b). The black dots indicate the saddle-point positions.

fluid may differ largely from a unitary Fermi gas near a broad MFR [5–7].

A. Stability of ^{173}Yb superfluid near OFR

The first nontrivial issue we encounter is that the out-phase-solution is not a local minimum of the mean-field grand potential $\Omega_{\text{MF}}(\Delta_o, \Delta_c)$. In Fig. 4, we show two contour plots of the grand potential (at $\delta = 0$ and at $\delta = \delta_{\text{res}}$). It is clear that the out-of-phase solution corresponds to a saddle point of the grand potential. The true ground state corresponds to the deep bound state with energy Z_- . In this state, the chemical potential is large and negative, $\mu \simeq Z_-/2$, and hence both two channels are in the deep BEC state. The BCS-BEC crossover state, which is an excited state, may suffer from some mechanical instabilities, such as negative compressibility. We have calculated the compressibility for ^{173}Yb system. Fortunately, the compressibility is always positive for the out-of-phase solution.

Next, we check whether the system suffers from any dynamical instability. Using the vertex function $\Gamma(Q)$, it is convenient to calculate the density excitation spectrum. The dispersions $\omega(q)$ are determined by the

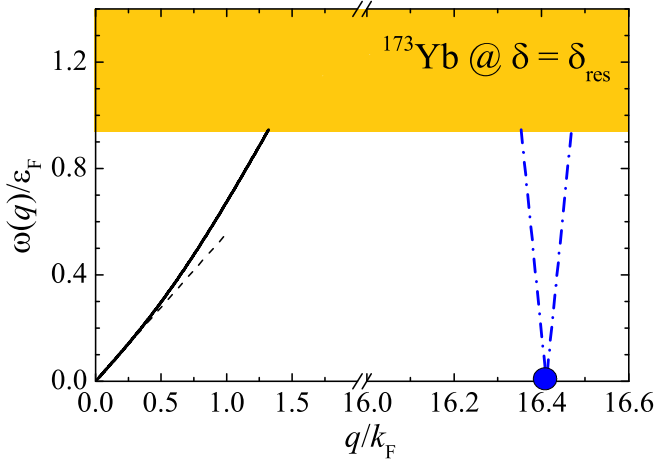


FIG. 5. (color online). In-gap density excitation spectrum of a ^{173}Yb Fermi gas at the resonance, which touches zero at a large momentum $q \gg k_F$ (the big blue dot). The dashed line plots the linear behavior $c_s q$ as $q \rightarrow 0$ characteristic of a sound wave. The colored area indicates the two-particle continuum.

pole of $\Gamma(\mathbf{q}, i\nu_l \rightarrow \omega + i0^+)$ after analytic continuation. Below the two-particle continuum, there are typically two modes corresponding to the in-phase and out-of-phase fluctuations of the phase of the two order parameters. The in-phase mode is the well-known gapless Bogoliubov-Anderson-Goldstone phonon mode, while the out-of-phase mode - predicted by Leggett long time ago - acquires a finite mass [26]. The observation of a long-lived Leggett mode remains elusive [27–29].

Fig. 5 reports the in-gap density excitation spectrum of ^{173}Yb atoms. The phonon mode, which behaves like $c_s q$ at small momentum, is clearly seen. However, we are unable to identify a well-defined gapped Leggett mode. Instead, an anomalous mode is observed at large momentum $q_A \simeq 16.4k_F$. It touches zero and causes an instability with respect to the density perturbation at the length scale $l \sim q_A^{-1} \simeq 5.3$ nm. The existence of such an anomalous mode is easy to understand. The out-of-phase solution of current interest is a saddle point solution and hence is intrinsically unstable. We have checked by varying parameters that the anomalous mode indeed appears as long as the out-of-phase solution is an excited state (see Fig. 1b). For the ^{173}Yb case, fortunately, we do not need to worry about this dynamical instability, since the nano scale of the density perturbation is too small to trigger experimentally. Theoretically, the instability also does not show up in our numerical calculations, as the pair fluctuation contribution decays exponentially fast with increasing momentum q . Therefore, we conclude that the BCS-BEC crossover in ^{173}Yb atoms with OFR is intrinsically metastable and can be realized in future experiments.

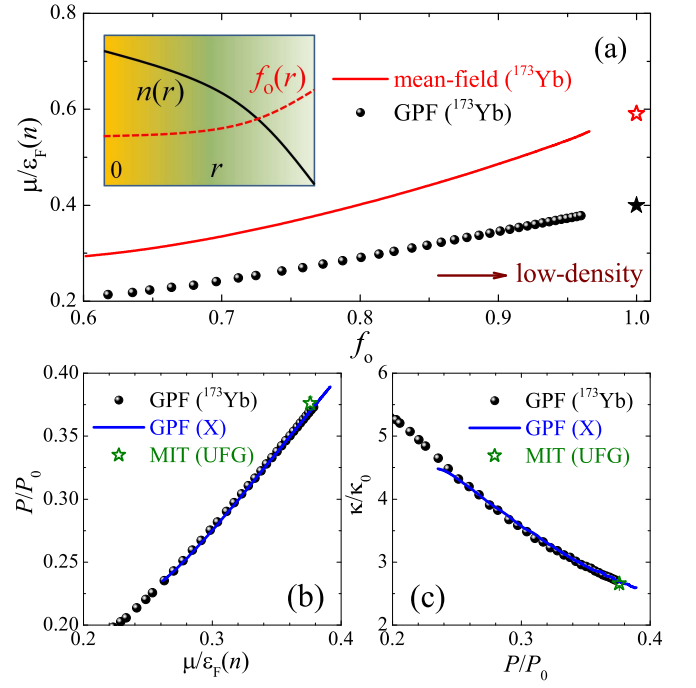


FIG. 6. (color online). (a) The chemical potential of a ^{173}Yb Fermi gas at the resonance, as a function of the open-channel fraction with decreasing density (see the inset for an experimental illustration in traps). In the low-density limit, where the population of the closed channel vanishes, the chemical potential approaches the prediction for broad Feshbach resonances (indicated by stars). Universal equations of state - pressure versus chemical potential (b) and compressibility versus pressure (c) - of the resonantly interacting ^{173}Yb Fermi gas. The circles are the result for ^{173}Yb atoms. The blue line (GPF-X) shows the result for a different set of interaction parameters. The stars show the MIT result for a unitary ^6Li Fermi gas (UFG) at broad Feshbach resonances [7]. The highest density in our calculations is about $n \sim 5 \times 10^{14} \text{ cm}^{-3}$.

B. EoS of ^{173}Yb superfluid at OFR

We now explore in greater detail a peculiar feature of the strongly interacting ^{173}Yb Fermi superfluid - a novel EoS - as a result of the key component of OFR, the large triplet scattering length a_{s+} . Near the resonance, the grand canonical equation of state, the pressure P as a function of the chemical potential μ at $T = 0$, can be expressed as

$$\frac{P(\mu)}{P_0(\mu)} = f_\mu \left[\frac{\mu}{\delta_{\text{res}}}; \frac{\delta}{\delta_{\text{res}}}, \frac{a_{s-}}{a_{s+}}, \{x_i\} \right]. \quad (59)$$

Here, $P_0(\mu) = (2M\mu)^{5/2}/(15\pi^2 M)$ and $\{x_i\}$ denotes collectively the other small interaction lengths such as the effective ranges $r_{s\pm}/a_{s+}$. For ^{173}Yb atoms, since the triplet scattering length a_{s+} is large, we may expect that the dependence on the small parameters a_{s-}/a_{s+} and x_i is rather weak. Hence at the resonance, the grand canon-

ical EoS depends only on the reduced chemical potential μ/δ_{res} ,

$$\frac{P(\mu)}{P_0(\mu)} \approx f_\mu \left(\frac{\mu}{\delta_{\text{res}}} \right). \quad (60)$$

On the other hand, we expect that in the low-density limit $n \rightarrow 0$, or explicitly $\varepsilon_F/\delta_{\text{res}} \rightarrow 0$, we recover the universal EoS of the two-component unitary Fermi gas, which has been realized by using the broad MFR [5–7]. We therefore consider the canonical EoS. The pressure can be expressed as

$$\frac{P(n)}{P_0(n)} = f_n \left[\frac{\mu(n)}{\varepsilon_F(n)}; \frac{\delta}{\delta_{\text{res}}}, \frac{a_{s-}}{a_{s+}}, \{x_i\} \right]. \quad (61)$$

For ^{173}Yb atoms, the dependence on the small parameters a_{s-}/a_{s+} and x_i is rather weak. At the OFR we have

$$\frac{P(n)}{P_0(n)} \approx f_n \left[\frac{\mu(n)}{\varepsilon_F(n)} \right], \quad (62)$$

where $P_0 = (2/5)n\varepsilon_F$. Therefore, the pressure depends only on a single parameter, the reduced chemical potential $\mu(n)/\varepsilon_F(n)$. This novel EoS can be easily measured experimentally. In harmonic traps, all the thermodynamic functions, in particular, the pressure and compressibility can be directly determined from measuring the local density [7, 39]. Away from the trap center, with decreasing density, the closed-channel fraction decreases to zero, due to the enlarged effective detuning, and the reduced chemical potential $\mu(n)/\varepsilon_F(n)$ then increases to reach the universal Bertsch parameter ξ in the broad MFR limit ($\xi \simeq 0.59$ in mean-field theory and $\xi \simeq 0.40$ in GPF theory [35, 36]), as shown in Fig. 6a. By varying slightly a_{s-}/a_{s+} and keeping δ_{res} invariant (i.e., the data labelled GPF-X in Figs. 6b and 6c), we have examined theoretically that both P/P_0 and κ/κ_0 , where $\kappa_0 = 3/(2n\varepsilon_F)$, indeed collapse onto a single curve. We note that, in the dilute limit ($n \rightarrow 0$), we recover the universal EoS of the two-component unitary Fermi gas. This universal EoS may be understood from the fact that in the dilute limit, the Zeeman splitting δ between the two channels becomes much larger than the Fermi energy ε_F . In this case, one can generally show that the closed-channel population becomes vanishingly small [33]. The strong coupling between the two channels ensures that we recover the universal EoS for the broad MFR case. However, this universal EoS may hardly be extended to the high density regime where $n \sim 10^{14} \text{ cm}^{-3}$.

C. Leggett Mode

We turn to consider the condition for the observation of the massive Leggett mode, by allowing a variable sin-

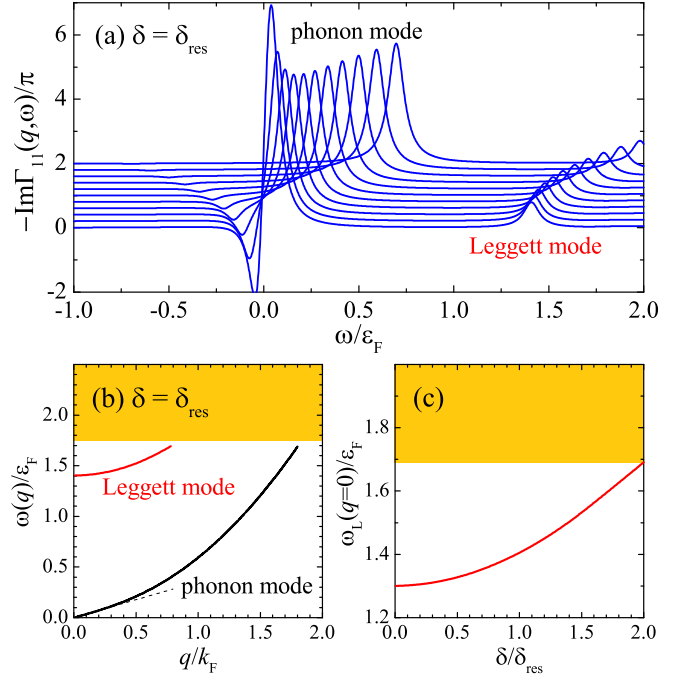


FIG. 7. (color online). (a) In-gap spectral function of Cooper pairs (in arbitrary units) at the resonance with the scattering lengths $a_{s+} = 1900a_0$ and $a_{s-} = 2a_{s+}$. From bottom to top, the momentum q increases from $0.1k_F$ to $1.1k_F$. The curves are vertically shifted for better illustration. A finite line width is included to broaden the δ -peak. (b) The corresponding in-gap density excitation spectrum. (c) The detuning dependence of the zero-momentum Leggett mode frequency $\omega_L(q=0)$. The colored area shows the two-particle continuum at $\delta = 2\delta_{\text{res}}$.

glet scattering length a_{s-} . It turns out that the out-of-phase solution of the two pairing parameters becomes the ground state once $1/(k_F a_{s-})$ is smaller than a threshold $1/(k_F a_{s-})_c = 1/(k_F a_{s+})$ (see Fig. 1b). It is easy to understand this threshold. Because $a_{s+} = a_{s-}$ at this threshold, the two channels decouples and hence the out-of-phase and in-phase solutions become degenerate.

We find that an undamped Leggett mode exists below the two-particle continuum when $|a_{s-}|$ is sufficiently large. In this case, we have two well-behaved condensates that satisfy Leggett's original picture for the appearance of the massive Leggett mode [26]. Fig. 7a shows a typical spectral function of the Green's function of the collective modes for $a_{s-} = 2a_{s+}$ and at $\delta = \delta_{\text{res}}$, where the Leggett mode is clearly visible. Its dispersion at small q can be well approximated by $\omega_L^2(q) \simeq \omega_L^2(0) + c_L^2 q^2$ (Fig. 7b). With increasing detuning (Fig. 7c) or decreasing $1/(k_F a_{s-})$, the Leggett mode is pushed upwards, and finally merges into the two-particle continuum. Experimentally, it is unclear whether we can find a realistic OFR system with both large singlet and triplet scattering lengths, which demonstrates the existence of the long-sought Leggett mode. If such a system can be found, the

Leggett mode can be probed by measuring the dynamic density structure factor via the Bragg spectroscopy [40].

V. SUMMARY

In summary, we calculated the OFR with realistic Lenard-Jones potentials and presented a low-energy effective theory for OFR which is useful for field theoretical study of the many-body system. We presented a strong-coupling pair fluctuation theory for the BCS-BEC crossover in ^{173}Yb atoms across its OFR. The stability of the BCS-BEC crossover, the equation of state at the OFR, and the collective modes (in particular the massive Leggett mode) are investigated by using the pair fluctuation theory. Since the BCS-BEC crossover in ^{173}Yb atoms corresponds to an excited state, there exists a dynamical instability with respect to an inhomogeneous density perturbation. Fortunately, due to the small singlet scattering length, this instability occurs at very large momentum and hence is hard to trigger under current experimental conditions. Hence the BCS-BEC crossover in ^{173}Yb atoms with OFR is intrinsically metastable and can be realized in future experiments. The small singlet scattering length in ^{173}Yb atoms also leads to a novel EoS, which is peculiar for a Feshbach resonance with sizable closed-channel fraction. The massive Leggett mode in the superfluid state of ^{173}Yb atoms is severely damped. We find that an undamped Leggett mode exists only for the case with both large singlet and triplet scattering lengths.

Our quantitative predictions could be experimentally examined in the near future in cold-atom laboratories [19, 20]. They also might be relevant to other two-band fermionic superfluids/superconductors in diverse fields of physics, such as MgB_2 and $\text{LaFeAsO}_{0.89}\text{F}_{0.11}$ in solid-state physics [41, 42].

We would like to thank Hui Zhai for useful discussions. This work is supported by the Thousand Yong Talent Program in China (LH), the ARC Discovery Projects: DP140100637 and FT140100003 (XJL), FT130100815 and DP140103231 (HH), and National Natural Science Foundation of China: Grant No.11474315 (SGP).

-
- [1] I. Bloch, J. Dalibard, and W. Zwerger, Many-body physics with ultracold gases, *Rev. Mod. Phys.* **80**, 885 (2008).
 - [2] C. Chin, R. Grimm, P. Julienne, and E. Tiesinga, Feshbach resonances in ultracold gases, *Rev. Mod. Phys.* **82**, 1225 (2010).
 - [3] S. Giorgini, L. P. Pitaevskii, and S. Stringari, Theory of ultracold atomic Fermi gases, *Rev. Mod. Phys.* **80**, 1215 (2008).
 - [4] W. Ketterle and M. W. Zwierlein, Making, probing and

- understanding ultracold Fermi gases, *Rivista del Nuovo Cimento* **31**, 247 (2008).
- [5] S. Nascimbène, N. Navon, K. J. Jiang, F. Chevy, and C. Salomon, Exploring the thermodynamics of a universal Fermi gas, *Nature (London)* **463**, 1057 (2010).
- [6] M. Horikoshi, S. Nakajima, M. Ueda, and T. Mukaiyama, Measurement of universal thermodynamic functions for a unitary Fermi gas, *Science* **327**, 442 (2010).
- [7] M. J. H. Ku, A. T. Sommer, L. W. Cheuk, and M. W. Zwierlein, Revealing the superfluid lambda transition in the universal thermodynamics of a unitary Fermi gas, *Science* **335**, 563 (2012).
- [8] K. Martiyanov, V. Makhalov, and A. Turlapov, Observation of a two-dimensional Fermi gas of atoms, *Phys. Rev. Lett.* **105**, 030404 (2010).
- [9] B. Fröhlich, M. Feld, E. Vogt, M. Koschorreck, W. Zwerger, and M. Köhl, Radio-frequency spectroscopy of a strongly interacting two-dimensional Fermi gas, *Phys. Rev. Lett.* **106**, 105301 (2011).
- [10] P. Dyke, E. D. Kuhnle, S. Whitlock, H. Hu, M. Mark, S. Hoinka, M. Lingham, P. Hannaford, and C. J. Vale, Crossover from 2D to 3D in a weakly interacting Fermi gas, *Phys. Rev. Lett.* **106**, 105304 (2011).
- [11] P. A. Murthy, I. Boettcher, L. Bayha, M. Holzmann, D. Kedar, M. Neidig, M. G. Ries, A. N. Wenz, G. Zurn, and S. Jochim, Observation of the Berezinskii-Kosterlitz-Thouless phase transition in an ultracold Fermi gas, *Phys. Rev. Lett.* **115**, 010401 (2015).
- [12] K. Fenech, P. Dyke, T. Peppler, M. G. Lingham, S. Hoinka, H. Hu, and C. J. Vale, Thermodynamics of an attractive 2D Fermi gas, *Phys. Rev. Lett.* **116**, 045302 (2016).
- [13] T.-L. Ho, Universal thermodynamics of degenerate quantum gases in the unitarity limit, *Phys. Rev. Lett.* **92**, 090402 (2004).
- [14] H. Hu, P. D. Drummond, and X.-J. Liu, Universal thermodynamics of strongly interacting Fermi gases, *Nature Phys.* **3**, 469 (2007).
- [15] P. A. Lee, N. Nagaosa, and X.-G. Wen, Doping a Mott insulator: Physics of high-temperature superconductivity, *Rev. Mod. Phys.* **78**, 17 (2006).
- [16] D. Lee and T. Schäfer, Cold dilute neutron matter on the lattice. I. Lattice virial coefficients and large scattering lengths, *Phys. Rev. C* **73**, 015201 (2006).
- [17] P. F. Kolb and U. Heinz, in: R. C. Hwa, X.-N. Wang (Eds.), *Quark-Gluon Plasma 3*, World Scientific, River Edge, NJ, 2004, p. 634.
- [18] R. Zhang, Y. Cheng, H. Zhai, and P. Zhang, Orbital Feshbach resonance in alkali-earth atoms, *Phys. Rev. Lett.* **115**, 135301 (2015).
- [19] G. Pagano, M. Mancini, G. Cappellini, L. Livi, C. Sias, J. Catani, M. Inguscio, and L. Fallani, Strongly interacting gas of two-electron fermions at an orbital Feshbach resonance, *Phys. Rev. Lett.* **115**, 265301 (2015).
- [20] M. Höfer, L. Riegger, F. Scazza, C. Hofrichter, D. R. Fernandes, M. M. Parish, J. Levinsen, I. Bloch, and S. Fölling, Observation of an orbital interaction-induced Feshbach resonance in ^{137}Yb , *Phys. Rev. Lett.* **115**, 265302 (2015).
- [21] The value of the resonance field $B_0 = 55 \pm 8\text{G}$ provided in Ref. [20] is for a finite temperature case, not the zero energy result.
- [22] Hui Zhai, private communication in January 2016.
- [23] M. Iskin, Two-band superfluidity and intrinsic Josephson

- son effect in alkaline-earth Fermi gases across an orbital Feshbach resonance, *Phys. Rev. A* **94**, 011604(R) (2016).
- [24] C.-H. Pao, S.-T. Wu, and S.-K. Yip, Superfluid stability in the BEC-BCS crossover, *Phys. Rev. B* **73**, 132506 (2006).
 - [25] L. He and P. Zhuang, Stable Sarma state in two-band Fermi systems, *Phys. Rev. B* **79**, 024511 (2009).
 - [26] A. J. Leggett, Number-phase fluctuations in two-band superconductors, *Prog. Theor. Phys.* **36**, 901 (1966).
 - [27] G. Blumberg, A. Mialitsin, B. S. Dennis, M. V. Klein, N. D. Zhigadlo, and J. Karpinski, Observation of Leggett's collective mode in a multiband MgB_2 superconductor, *Phys. Rev. Lett.* **99**, 227002 (2007).
 - [28] S.-Z. Lin and X. Hu, Massless Leggett mode in three-band superconductors with time-reversal-symmetry breaking, *Phys. Rev. Lett.* **108**, 177005 (2012).
 - [29] N. Bittner, D. Einzel, L. Klam, and D. Manske, Leggett Modes and the Anderson-Higgs mechanism in superconductors without inversion symmetry, *Phys. Rev. Lett.* **115**, 227002 (2015).
 - [30] J. Xu, R. Zhang, Y. Cheng, P. Zhang, R. Qi, and H. Zhai, arXiv:1602.06513 (2016).
 - [31] S. G. Porsev, M. S. Safronova, A. Derevianko, and C. W. Clark, Long-range interaction coefficients for ytterbium dimers, *Phys. Rev. A* **89**, 012711 (2014).
 - [32] K. L. Baluja, P. G. Burke, L. A. Morgan, R-matrix propagation program for solving coupled second-order differential equations, *Comput. Phys. Commun.* **27**, 299 (1982).
 - [33] L. He, X.-J. Liu, and H. Hu, Two-band description of resonant superfluidity in atomic Fermi gases, *Phys. Rev. A* **91**, 023622 (2015).
 - [34] C. A. R. Sá de Melo, M. Randeria, and J. R. Engelbrecht, Crossover from BCS to Bose superconductivity: Transition temperature and time-dependent Ginzburg-Landau theory, *Phys. Rev. Lett.* **71**, 3202 (1993).
 - [35] H. Hu, X.-J. Liu, and P. D. Drummond, Equation of state of a superfluid Fermi gas in the BCS-BEC crossover, *Europhys. Lett.* **74**, 574 (2006).
 - [36] R. B. Diener, R. Sensarma, and M. Randeria, Quantum fluctuations in the superfluid state of the BCS-BEC crossover, *Phys. Rev. A* **77**, 023626 (2008).
 - [37] L. He, H. Lu, G. Cao, H. Hu, and X.-J. Liu, Quantum fluctuations in the BCS-BEC crossover of two-dimensional Fermi gases, *Phys. Rev. A* **92**, 023620 (2015).
 - [38] G. Bighin and L. Salasnich, Finite-temperature quantum fluctuations in two-dimensional Fermi superfluids, *Phys. Rev. B* **93**, 014519 (2016).
 - [39] T.-L. Ho and Q. Zhou, Obtaining phase diagram and thermodynamic quantities of bulk systems from the densities of trapped gases, *Nature Phys.* **6**, 131 (2010).
 - [40] M.G. Lingham, K. Fenech, S. Hoinka, and C. J. Vale, Local observation of pair condensation in a Fermi gas at unitarity, *Phys. Rev. Lett.* **112**, 100404 (2014).
 - [41] X. X. Xi, Two-band superconductor magnesium diboride, *Rep. Prog. Phys.* **71**, 116501 (2008).
 - [42] F. Hunte, J. Jaroszynski, A. Gurevich, D. C. Larbalestier, R. Jin, A. S. Sefat, M. A. McGuire, B. C. Sales, D. K. Christen, and D. Mandrus, Two-band superconductivity in $\text{LaFeAsO}_{0.89}\text{F}_{0.11}$ at very high magnetic fields, *Nature (London)* **453**, 903 (2008).